

Effects of van der Waals interaction on the N₂ adsorption on carbon nanotubes: proposal of new force field parameters

Carlos Alberto Martins Junior,^{*,†} Henrique Musseli Cezar,^{*,†,‡} Daniela Andrade Damasceno,^{*,†} and Caetano Rodrigues Miranda^{*,†}

[†]*Universidade de Sao Paulo, Instituto de Fisica, Rua do Matao 1371, Sao Paulo, SP, 05508-090, Brazil*

[‡]*Hylleraas Centre for Quantum Molecular Sciences and Department of Chemistry, University of Oslo, PO Box 1033 Blindern, 0315 Oslo, Norway*

E-mail: camjir.cm@usp.br; h.m.cezar@kjemi.uio.no; daniela.damasceno@usp.br; crmiranda@usp.br

Abstract

The separation of carbon dioxide (CO₂) from nitrogen gas (N₂), the main component of flue gas, has become an emerging action to mitigate climate change. Feasible and efficient approaches to exploring the separation properties of materials are molecular dynamics (MD) and Monte Carlo (MC) simulations. In these approaches, a careful choice of force fields is required to avoid unrealistic predictions of thermodynamic properties. However, most studies use Lorentz-Berthelot combining rules (LB) to obtain the interaction between different species, an approximation that could not capture the essence of interfacial interactions. In this context, we verified how accurate LB is in describing the interaction of N₂ molecules and

carbon nanostructures by comparing the interaction energies from LB with those from density functional theory (DFT) calculations. We selected carbon nanomaterials because they are considered promising materials to perform N_2/CO_2 separation. The results show that the LB underestimates the interaction energies and affects the prediction of fundamental properties of solid-fluid interfacial interactions. To overcome this limitation, we parametrized a Lennard-Jones potential using energies and forces from DFT, obtained through the van der Waals functional KBM. The proposed potential show good transferability and agreement to *ab-initio* calculations. Grand Canonical Monte Carlo simulations were performed to verify the effects of employing LB in predicting the amount of nitrogen gas adsorbed inside different CNTs. LB predicts a lower density inside them. Moreover, our results suggest that LB leads to a different characterization of the adsorption properties of carbon nanotubes, by changing significantly the adsorption isotherm.

Introduction

One of the most studied approaches to mitigate carbon dioxide emission (CO_2) is Carbon Capture and Storage (CCS),¹ which consists of capturing greenhouse gases from the combustion of fossil fuels and storing it in geological formations. However, to perform CCS, it is necessary to efficiently separate CO_2 from other molecules that compose flue gases. These gases are mainly composed of nitrogen gas (N_2),^{2,3} which has driven several studies to improve the separation process of this gas from carbon dioxide.⁴

A class of materials that possesses desirable properties for gas separation application is carbon nanostructures.^{5,6} They are mechanically and chemically stable^{7,8} and, besides that, their properties can be easily tuned by functionalization, i.e., by incorporating some radicals in the structures,⁶ or by doping it.⁹ For example, studies have found that functionalized multi-walled carbon nanotubes enhance the separation properties of mixed matrix membranes.¹⁰ In another study, experiments showed that nanoporous graphene (NPG) separates

different gases,¹¹ which boosted the investigation of the separation properties of NPGs. For instance, in the case of N₂/CO₂ separation, nanoporous with different diameters and geometries were tested.^{12,13} Moreover, different atoms were used to passivate the nanoporous rim.^{12,14} These studies have shown that NPGs can efficiently perform the N₂/CO₂ separation, reaching a selectivity of 100%.

Feasible and efficient approaches to study gas separation are Molecular Dynamics or Monte Carlo simulations. In these types of molecular modeling, the interactions between different species are usually obtained by a Lennard-Jones potential,

$$V(r) = 4\epsilon \left[\left(\frac{\sigma}{r} \right)^{12} - \left(\frac{\sigma}{r} \right)^6 \right] \quad (1)$$

in which the ϵ and σ parameters are given by averaging the parameters that describe the isolated species. A common way of performing such averages is through the Lorentz-Berthelot combination rules (LB), $\sigma_{ij} = (\sigma_{ii} + \sigma_{jj})/2$ and $\epsilon_{ij} = \sqrt{\epsilon_{ii}\epsilon_{jj}}$, in both of which the sub-index ij refers to the cross interaction while ii and jj refer to the pure species. Although LB are widely employed, different studies have shown that it may not capture the essence of interfacial interactions.^{15,16}

In the case of N₂ interacting with graphene, there is at least one force field that goes beyond LB: Vekeman *et al.* proposed new parameters derived from density functional theory (DFT) calculations.¹⁷ However, the chosen functional, B97-D, is known to significantly deviate from coupled clusters calculations (CCSD(T)), which is considered to fully describe van der Waals interactions. For example, a deviation of 18.25% was found for coronene adsorbed on graphene.¹⁸ Recent studies confirm the accuracy of van der Waals functionals, such as KBM and C09,^{19,20} to describe adsorption energies. For instance, results show that the adsorption energy of CO₂ on graphene obtained from both functionals agree with experimental results.^{15,21} In particular for N₂ and carbon nanomaterials, such functionals should be employed since vdW forces are the main interaction.²² Besides the functional, another

consideration taken in the study performed by Vekeman *et al.* that might affect the final results is the use of a finite size material to perform the calculations instead of using a graphene sheet. This was probably done due to a limitation of the used software. However, the finite size and strategies used to passivate the border of the material that mimics graphene may affect the adsorption energies.

Based on the above review of the literature, we compared the adsorption energy curves of N_2 molecules on carbon structures obtained from different classical force fields (FFs) using LB rules with the ones from DFT calculations using the KBM functional. A large discrepancy between results from LB and DFT was observed, which imposed a need for developing a precise potential with a new set of cross parameters for the N–C and N–H interactions. The proposed potential showed high accuracy in describing the adsorption energy of N_2 molecules on graphene and carbon nanotubes compared to DFT. To verify the effects of the underestimation of the vdW interactions on the thermodynamics properties, we performed Monte Carlo simulations to obtain the load of N_2 inside carbon nanotubes, at 300 K and 1 atm, and the adsorption isotherm at 300 K. The results reveal that LB underestimates the load, independent of force field used to obtain the interaction, and change the adsorption properties, since the isotherms obtained from the proposed potential are significantly different to the one obtained through LB. These findings indicate that LB might not be adequate for the full description of the interaction of different species when vdW forces play an important role, as in the case of N_2 and carbon nanomaterials, and lead to results inconsistent with those obtained with electronic dispersion and experiments present in the literature.

Methods and Models

Carbon Nanostructures

We considered the following carbon nanostructures: a 5×5 graphene sheet and $(m, n) = (8, 8), (10, 10), (0, 17)$ carbon nanotubes. These structures were created using the VMD soft-

ware²³ and the Topotools plug-in.²⁴ It was decided not to optimize the other nanostructures to match the bond lengths with those from the classical force fields. For the N₂ bond length, we used a value of 1.10 Å, while for the carbon nanomaterials, bond lengths were considered to be 1.418 Å.

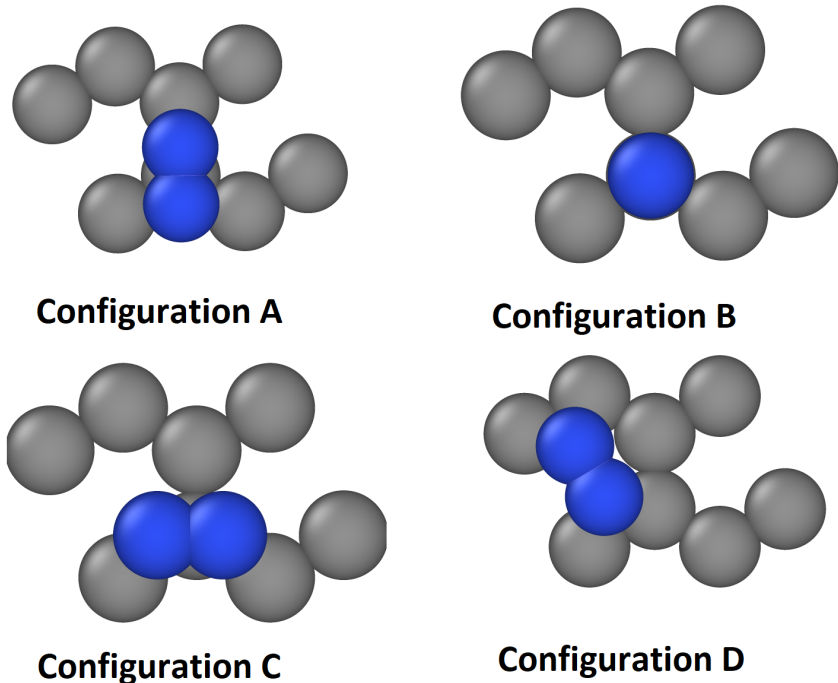


Figure 1: Adsorption configurations considered in the calculations. For clarity, these images show a nitrogen molecule adsorbed on a 2×2 graphene cell. The gray spheres represent the carbon atoms, the blue ones represent the nitrogen atoms, and the white ones represent the hydrogens. The visualizations were generated using Ovito.²⁵

Classical Force Fields

To determine the accuracy of LB combination rules in describing the interaction between N₂ and carbon nanostructures, we compared the interaction energies obtained using different classical FFs with those from DFT calculations. We used the AIREBO,²⁶ Amber,²⁷ Mao,²⁸ Huang,²⁹ Steele,³⁰ and Walther³¹ force fields for the carbon structures and the Trappe model for N₂. They all use the Lennard-Jones potential, with ϵ_{ii} and σ_{ii} presented in Table 1. We selected only a model for N₂ due to the small differences in the force field parameters of

different models, as can also be seen in table 1. The interaction energies were obtained in four different adsorption sites. The adsorption configurations are represented in figure 1.

Table 1: Force field parameters for carbon structures (first part of the table) and nitrogen molecules (second part of the table). All force fields for N_2 studied here are three-site models. In such models, two sites are localized in each nitrogen atom while the other is localized at the center of the molecule. The charge q_i is the value at the nitrogen atoms. For the site at the center of the molecule, the charge is $-2q_i$.

Force Field	$\epsilon(K)$	$\sigma (\text{\AA})$	$q_i(e)$
AIREBO ²⁶	32.96	3.400	-
Amber ²⁷	43.30	3.400	-
Mao ²⁸	48.78	3.370	-
Huang ²⁹	35.26	3.550	-
Steele ³⁰	28.00	3.400	-
Walther ³¹	52.87	3.851	-
Trappe ³²	36.00	3.31	-0.482
Garcia-Perez ³³	36.40	3.32	-0.40484
Vujíc ³⁴	40.24	3.32	-0.482
Murthy ³⁵	36.44	3.33	-0.482

DFT calculations

DFT calculations were performed using the KBM exchange-correlation functional.¹⁹ This functional was found to successfully describe different systems in which the main interaction is due to van der Waals forces,^{19,36} as for N_2 molecules interacting with carbon materials.²² Furthermore, recent studies have shown that the KBM functional gives good results for the adsorption energy of CO_2 molecules on graphene, a system similar to the one investigated here.^{15,21} We also tested other vdW and non-vdW functionals, namely, the C09²⁰ and BH,³⁷ an LDA functional, PW92,³⁸ and a GGA functional, PBEsol.³⁹ These tests did not show a significant difference between the vdW functionals, with the largest difference in the depth of the well being from KBM to C09, 0.4424kcal/mol (7.2%). However, some significant differences were found from the vdW functionals to PW92 and PBEsol (see Figure S1 in the Supporting Information). Even though the LDA functional can describe the depth of

the interaction energy, when compared to the vdW functionals, it cannot describe all the features of the interaction energies curves. These tests also show that GGA - PBEsol cannot describe either the depth of the interaction curve or the other parts. This pattern indicates the importance of including electron dispersion when studying such systems.

We used a plane-wave cutoff of 400 Ry for the grid and a convergence criterion of 10^{-4} in the elements of the density matrix. The selected basis was a double zeta plus polarization orbitals, with the second zeta carrying 0.35 of the norm. Based on convergence tests, we selected an $8 \times 8 \times 1$ k-points grid for the single-point calculations involving the 5×5 graphene sheet and $1 \times 1 \times 1$ k-point for the CNTs. All the DFT calculations considered periodic boundaries conditions. Thus, to avoid interaction between the images of the system, the distance between the graphene sheets was 50 \AA and the CNTs were placed in the center of a $20 \text{ \AA} \times 20 \text{ \AA}$ plane. We also tested the convergence of the interaction energy on the length of the carbon nanotubes, which is present in Figure S2 of the Supporting Information. Based on these calculations, a length of 7.368 \AA was selected for the arm-chair nanotubes and 8.508 \AA for the zig-zag nanotube. All the dft calculations were performed using the SIESTA code REF.

The interaction energies from DFT were obtained using Eq. 2. The term E_{int} is the interaction energy, E_{sys} is the energy of the whole N_2 /carbon-nanomaterial system, E_c and E_{N_2} are the energies of the isolated carbon nanomaterial and isolated N_2 molecule, respectively.

$$E_{\text{int}} = E_{\text{sys}} - E_c - E_{\text{N}_2} \quad (2)$$

Classical Molecular Simulations

The interaction energies for the classical force fields were obtained using LAMMPS,⁴⁰ and the Moltemplate software⁴¹ was used to create the inputs. The energies were calculated using the compute group/group command, which does not include the interactions between the periodic images. Consequently, there was no need to test the convergence of the adsorption

energy on CNT length, as we did for the DFT calculations. Also, since we used classical force fields that use Lennard-Jones potential, which is a pairwise potential, an effect due to many-body interactions between the periodic images does not exist, as might happen in the DFT calculations.

Grand canonical Monte Carlo (GCMC) simulations were performed using the Cassandra software⁴² in order to obtain the N₂ density inside different carbon nanotubes using the force fields tested here and the fitted potential. To obtain the chemical potential of N₂ at 300.0 K and 1.0 atm, we used the Widom insertion method.⁴³ These simulations were carried for 4×10^6 MC steps, with the last 3×10^6 steps being considered for the production phase. Then, using the obtained chemical potential we performed GCMC simulations to load 200 Å long CNTs with N₂. Four different CNTS were considered: (6,6), (8,8), (10,10) and (12,12). Initially, 5×10^4 simulation steps in the NVT ensemble were performed to obtain the initial configuration. Then, a GCMC simulation of 5×10^6 MC steps was performed, in which molecules were translated, rotated, inserted, or deleted inside the carbon nanotubes with a 25% probability for each move. For this last simulation, we employed configurational-biased insertions with 16 trial insertions. A cutoff of 15 Å was used for the Lennard-Jones plus Coulomb potential along with the Ewald method for long-range electrostatics, in which accuracy of 10^{-5} was selected.

To verify the effects of the different force fields on adsorption properties, we also used GCMC simulations to obtain adsorption isotherms of CNT (10,10) and (0,17) at $T = 300$ K, using the Steele's, Walther's and the fitted force field. We selected the Steele force field since it predicts the smallest density on CNT (10,10), as can be seen in the Section Results. For these simulations, we first simulated bulk N₂ with different chemical potentials at the GCMC ensemble to obtain the average value of pressure. Simulations of 3.5×10^6 MC steps were performed to reach the equilibrium and, then, 3×10^6 MC steps were performed for the production phase. We used a tail correction for the simulations of the bulk, while the other simulations parameters were the same as previously discussed. Then, other simulations were

performed to insert N₂ molecules inside the carbon nanotubes. With these last simulations, we matched the number of adsorbed molecules inside the CNTs to the bulk pressure, obtaining the adsorption isotherm. Aside from the tail correction, we used the same simulation parameters. For the calculations of the gas density, we used the accessible volume, which was found by monitoring the position of nitrogen atoms inside the CNTs.

Fitting Procedure

Due to the difference between the energy curves from the DFT calculations and LB rules (see the Results section), we fitted a new set of Lennard-Jones parameters for the interactions between nitrogen and (10,10) and (0,17) CNTs interfacial interactions using GULP.⁴⁴ To better fit the minimum of the energy curves, a weight based on the Boltzmann distribution was used,

$$w = e^{\frac{E-E_{\min}}{kT}} \quad (3)$$

in which w is the weight, E_{\min} is the minimum of the curve, k is the Boltzmann constant, and $T = 350$ K is the temperature. It is worth mentioning that T does not hold a physical meaning and is just used to obtain a better description around the curve minimum. We also added another weight to the energies to balance the fact that the number of forces is greater since there are $3N$ forces components, being N the number of atoms, for each point in the interaction energy curve. The temperature and energy weight were selected by manually checking how well the fitting was compared to DFT energies and forces.

Results and Discussion

Comparison between DFT and FFs

Figure 2 shows the adsorption energies curves obtained with DFT, the classical force fields using LB combination rules, and the proposed potential. These results indicate that the

classical force fields underestimate the interaction energy between the nitrogen molecule and graphene or carbon nanotubes. Neither the position nor the depth of the potential wells are properly described. Since the parameters for both isolated systems can describe their interactions, we attribute this discrepancy to LB combination rules. These rules are an approximation, and there is no guarantee they can be used to successfully describe interfacial interactions.

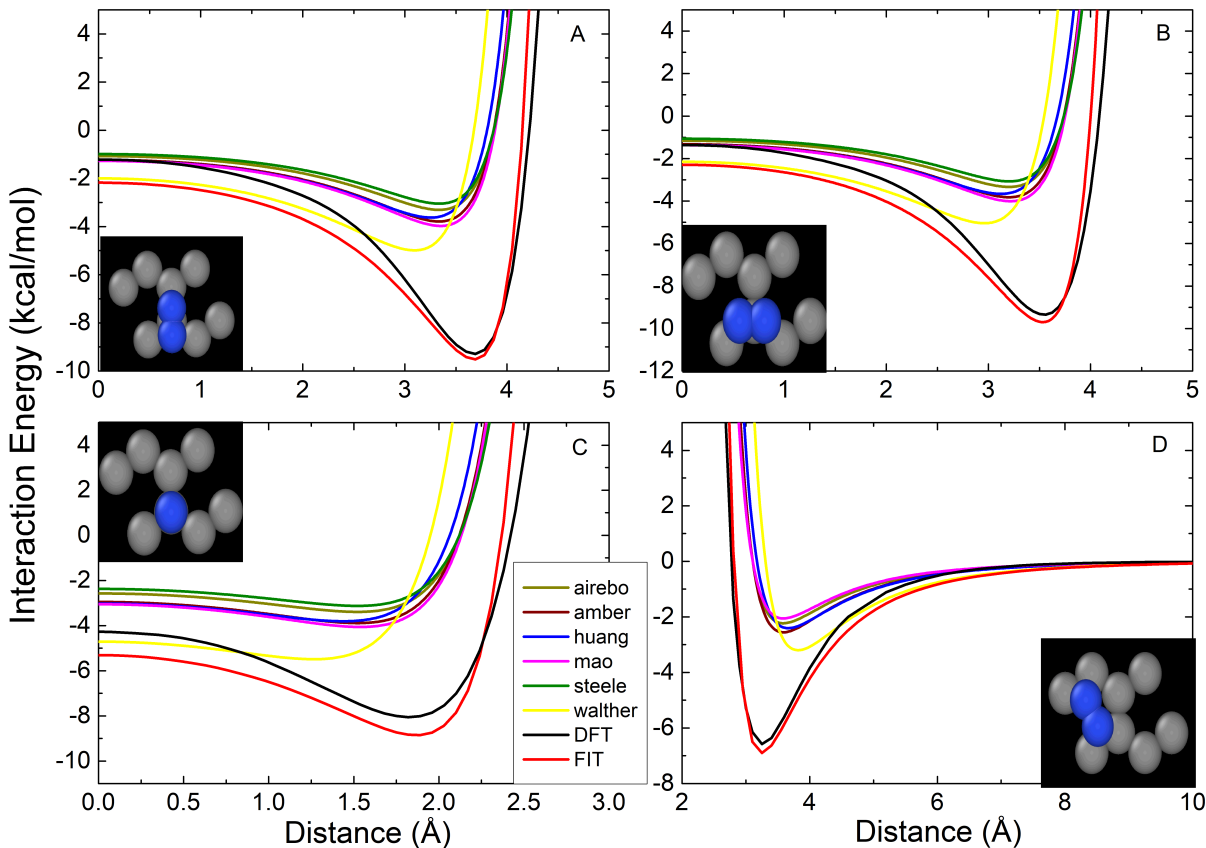


Figure 2: A) (10,10) CNT, B) (0,17) CNT, C) (8,8) CNT, and D) graphene. Comparison of the interaction energies of N₂ and different carbon nanostructures, using DFT-KBM, fitted LJ parameters, and classical forces fields through Lorentz-Berthelot combination rules. The fitting was performed using data from the (10,10) and (0,17) CNTs. The curves for graphene and the (8,8) CNT show the transferability of the potential to both smaller and larger curvatures.

The results also indicate that the adsorption site B (see Figure 1) is energetically the least favorable configuration and, aside from it, only slight differences between the other adsorption curves were observed, indicating no clear preferable adsorption site. A similar

result was reported in the literature. Using molecular dynamics simulations, Vekeman *et al.* has recently shown that if the flexibility of the graphene sheet is taken into account, a united-atom model for nitrogen molecules gives almost the same results as an atomistic model.⁴⁵ This suggests that the effect of orientation of nitrogen molecules is negligible. Moreover, it is possible to conclude that vdW interaction does not play a role in the orientation since the results from KBM and their results, derived from the B97-D functional,¹⁷ which does not include electron dispersion, give the same result for non-preferable orientation of N₂ molecules on graphene.

Some significant differences in the adsorption energy from our DFT calculations and others reported in the literature were found. Here, it was found an adsorption energy of -6.6 kcal/mol of N₂ on graphene, while a value of -2.6 kcal/mol was reported using the B97-D functional¹⁷ and a value of -3.2 kcal/mol was reported using ω B97X-D/cc-pVDZ.⁴⁶ We attribute these differences to the different levels of calculation employed in each work. First, in the cited studies, periodic boundary conditions were not used, which might affect the adsorption energies, since the finite size and strategies used to passivate the graphene border may affect the results. Second, it is known that the methodology employed in such studies leads to energies that are different from the ones obtained with coupled clusters calculations (CCSD(T)), which fully describes van der Waals interactions.⁴⁷ For example, a deviation of 18.25% between DFT - B97-D and CCSD(T) was observed for coronene adsorbed on graphene.¹⁸ Furthermore, the KBM exchange-correlation functional employed here was found to successfully describe the adsorption energy of carbon dioxide on graphene^{15,21}

Unfortunately, based on the authors' knowledge, there are no experimental data for N₂ adsorption energies on graphene, as in the case of CO₂. The only experimental results available are for the adsorption energy of N₂ on graphite, in which values of -2.236 to -2.624 kcal/mol have been reported for the depth of the well.⁴⁸ However, the adsorption energy on graphite can be significantly different from graphene.^{15,21}

Fitting

Due to the reported underestimation of the adsorption energies, we performed a fit of the Lennard-Jones cross parameters. As described in the methodology, we used only forces and energies from the (10,10) and (0,17) CNTs in the fitting process. The fitted LJ cross parameters are shown in Table 2. Figure 2 shows curves for the interaction energies obtained from DFT, the fitted potential, and classical forces fields employing the Lorentz-Berthelot combination rules. The results show that the differences between the proposed fit and the DFT calculations are smaller than 1.0 kcal/mol, which is within the chemical accuracy. Extending the application to other models, including graphene and (8,8) CNT, the results indicate that the fit is transferable for both smaller and larger curvatures.

Table 2: Fitted Lennard-Jones parameters for N–C interactions.

	ϵ_{ij} (K)	σ_{ij} (Å)
N–C	118.82	3.011

Figure 3 compares forces acting on selected atoms using fitted parameters and DFT calculations. Overall, the curves are in reasonable agreement. The major discrepancies in forces are when the nitrogen molecule is near the carbon atoms, as shown in Figures 3-b and 3-c. As expected, at such short distances, the interactions are energetically unfavorable, leading to a low probability of visiting those points in the phase space during a simulation. For example, at 2.5 Å from the center of the (8,8) nanotube, when the fit starts to diverge from DFT (Figure 3-C), the interaction energy is 2.56 kcal/mol, while the lowest energy at the same adsorption configuration is -8.02 kcal/mol. Despite describing the force on nitrogen atoms, the fit could not reproduce all the features of the forces on carbon atoms. However, the difference is small and might not lead to distinct results in molecular dynamics simulations due to the thermal movement and the larger contribution of bonded forces acting on such atoms. The oscillation present in the forces from DFT is due to the eggbox effect present in our DFT calculations.⁴⁹

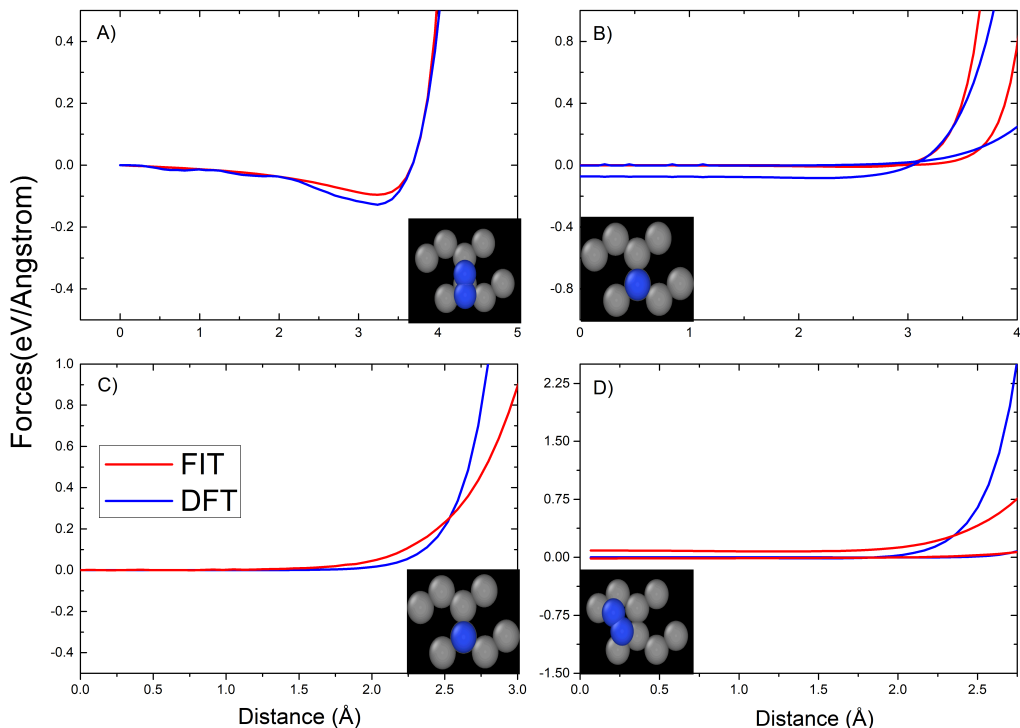


Figure 3: Figures A and C show the component of the force on a N atom in the direction that N₂ is moving towards the carbon atoms. Figures B and D show the components of the force on a C atom in the other directions. Figures A and B are from CNT(10,10) while figures C and D are from CNT(8,8). All figures show the comparison of the forces between N₂ and carbon nanostructure, using DFT-KBM and our fitted LJ parameters.

Grand Canonical Monte Carlo Simulations

Figure 4 compares the density of nitrogen molecules inside different CNTs, using classical force fields with LB and the proposed potential. Each FFs predicts a different density, illustrating the importance of a careful selection of the most appropriate force field for molecular simulations. For all the nanotube diameters, our fit predicts a larger number of nitrogen molecules, reaching an almost 40 fold difference for the (12,12) CNT compared to Steele's potential, respectively. The higher number of adsorbed molecules predicted by the fit can be related to the largest depth of the potential well of the carbon-nitrogen interaction and the σ , which is the distance where the potential is zero, being the smallest. Since our

fit agrees with DFT - KBM results, we suggest that the use of classical force fields and Lorentz-Berthelot combination rules underestimate the vdW interaction between a nitrogen molecule and carbon nanotubes, predicting different results than those obtained with a good vdW description.

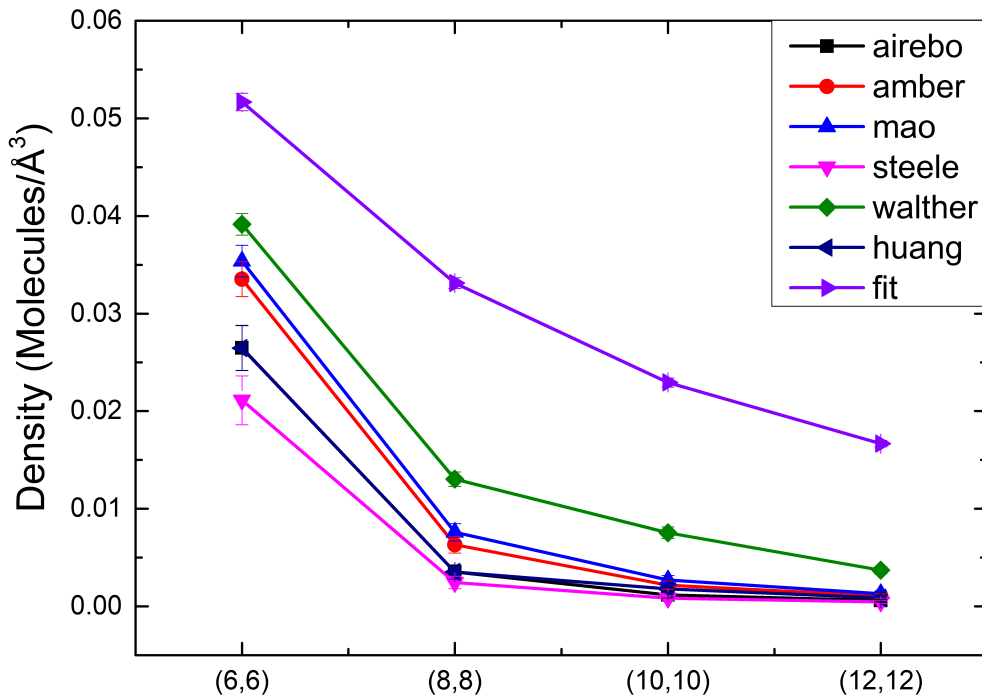


Figure 4: Comparison of the density of nitrogen molecules inside a (6,6), (8,8), (10,10) and (12,12) carbon nanotubes. The proposed potential predicts a larger number of molecules inside the nanotubes in all cases.

Figure 5 shows the isotherms of CNT (10,10) and (0,17), which have similar radius, obtained using the fitted, Steele’s and Walther’s potential. There is only small difference between the isotherms of CNT(10,10) and CNT(0,17), indicating that chirality does not play a role in the adsorption properties of carbon nanotubes. The difference is probably due to the slight differences in the volume of the CNTs.

Following the procedure described in Kumar *et al.*,⁵⁰ each potential predicts a different

isotherm curve, described by a different isotherm model. As can be seen in Figure S3, the isotherms predicted by the Steele potential are modeled by a Langmuir isotherm given by equation 4,

$$q_h = \frac{NKP}{1 + KP} \quad (4)$$

in which q_h is the concentration of adsorbed molecules, N is the number of adsorption sites, K is related to the binding energy, and P is the pressure. The isotherm predicted from Walther’s potential is modeled by a combination of Langmuir equations, as can be seen in the plot of a Scatchard equation on Figure S4. The proposed potential predicts that the isotherms are modeled by a Freundlich isotherm, as shown in Figure S5 of the supporting information, which agrees with experimental data in the literature.⁵¹⁻⁵³ The Freundlich model for adsorption isotherms is written in equation 5.

$$q_h = q_m b P^n \quad (5)$$

The term q_m is the maximum adsorption capacity, and b is an isotherm constant.⁵⁰

The reason for each potential predicts a different isotherm model might be the underestimation of the difference on the adsorption energies of different adsorption sites, since a single Langmuir equation predicts only a adsorption energy, while the Freundlich predicts a distribution. Indeed, the difference in energy between configuration A and C predicted from Steele’s potential is 0.002 kcal/mol, while the difference from the fitted potential is 0.19 kcal/mol, both of which below the thermal energy at room temperature (0.593 kcal/mol). Therefore, the results suggest that the underestimation of the adsorption energy from the LB combination rules also leads to an underestimation of the energy difference among the different adsorption sites, changing the adsorption properties of a material.

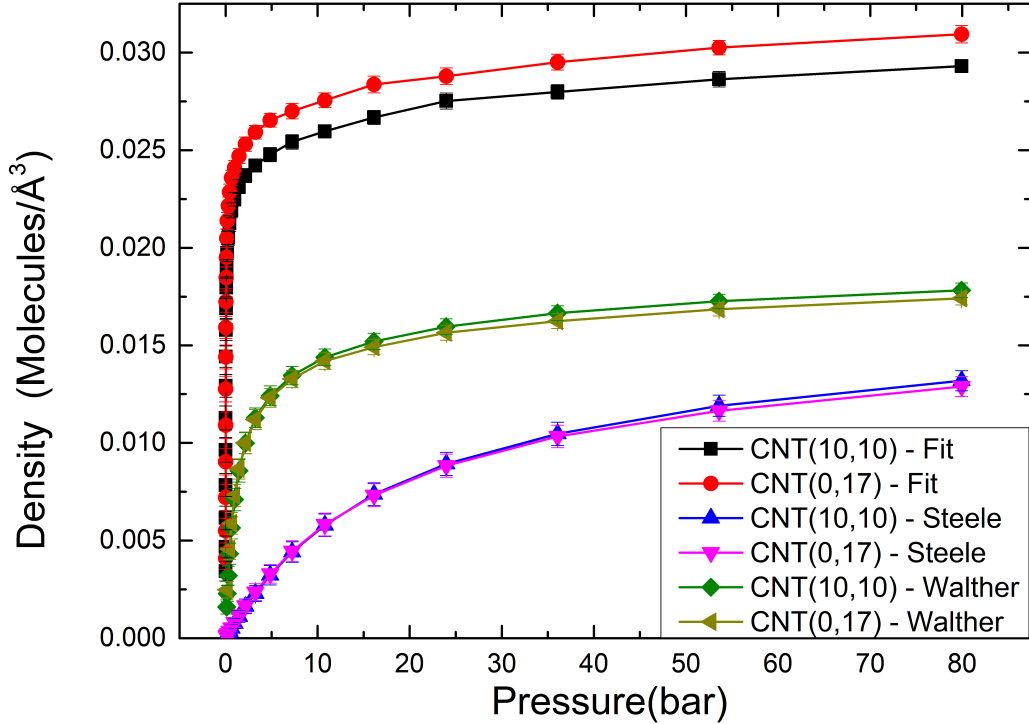


Figure 5: Adsorption isotherms of N_2 in the (10,10) and (0,17) CNTs, predicted by Steele potential and LB and by the proposed potential. The y-axis is the number of adsorbed molecules inside the simulated CNTs and this number is higher for the fitted potential, due to the larger potential depth.

Conclusion

In this work, we used DFT with vdW to describe the interactions between N_2 with graphene and carbon nanotubes. The comparison of the interaction between nitrogen molecules and carbon nanomaterials obtained through Lorentz-Berthelot combination rules and DFT - KBM calculations show that they underestimate the energies regardless of the potential used for the carbon nanostructures. Because of this underestimation, we fitted a new Lennard-Jones potential. The potential, derived from data from DFT, was aimed to describe N_2 interaction with carbon atoms on graphene and carbon nanotubes. We tested the difference of our proposed potential and Lorentz-Berthelot combination rules on the number of nitrogen

molecules inside arm-chair CNTs of different diameters and on the adsorption isotherms. These results suggest that Lorentz-Berthelot rules underestimate the load, making the results obtained using such approximation to be correspondent to those of a lower temperature or lower pressure. Moreover, they also indicate that LB predicts a different curve for the adsorption isotherm due to the underestimation of the difference in adsorption energies, leading to divergent adsorption properties. The parametrizations brought can help in the improvement of the accuracy of molecular simulations in which N_2 molecules are interacting with carbon nanostructures, such as simulations of gas separations.

Acknowledgments

CAMJ thanks CAPES for the PhD scholarship. The authors gratefully acknowledge the support of the RCGI – Research Centre for Gas Innovation, hosted by the University of São Paulo (USP) and sponsored by FAPESP – São Paulo Research Foundation (2014/50279-4, 2020/15230-5, and project number 2020/01558-9) and Shell Brasil, and the strategic importance of the support given by ANP (Brazil’s National Oil, Natural Gas, and Biofuels Agency) through the R&D levy regulation. The authors also acknowledge National Council for Scientific and Technological Development (CNPq) through grant 307064/2019-0 for financial support. HMC thanks to the financial support of FAPESP, grants #2019/21430-0 and #2017/02317-2, and the Research Council of Norway through the Centre of Excellence *Hylleraas Centre for Quantum Molecular Sciences* (grant number 262695). The computational time for the calculations was provided by High-Performance Computing facilities at the University of de São Paulo (USP).

Supporting Information

The Supporting Information of this work can be found online.

References

- (1) Gibbins, J.; Chalmers, H. Carbon capture and storage. *Energy Policy* **2008**, *36*, 4317–4322.
- (2) Granite, E. J.; Pennline, H. W. Photochemical Removal of Mercury from Flue Gas. *Energy Policy* **2002**, *41*, 5470–5476.
- (3) Park, S.-E.; Chang, J.-S.; Lee, K.-W. *Carbon Dioxide Utilization for Global Sustainability*; Elsevier, 2003.
- (4) Chawla, M. et al. Membranes for CO₂ /CH₄ and CO₂/N₂ Gas Separation. *Chemical Engineering and technology* **2007**, *43*, 184–199.
- (5) Sanip, S. M.; Ismail, A. F.; P.S.Goh; Norrdin, M.; T.Soga; Tanemura, M.; H.Yasuhiko Carbon Nanotubes Based Mixed Matrix Membrane for Gas Separation. *Advanced Materials Research* **2011**, *364*, 272–278.
- (6) Sanip, S. M.; F., I. A.; Goh, P. S.; Soga, T.; Tanemura, M.; Yasuhiko, H. Gas separation properties of functionalized carbon nanotubes mixed matrix membranes. *Separation and Purification Technology* **2011**, *78*, 208–218.
- (7) Yan, L.; Zheng, Y. B.; Zhao, F.; Li, S.; Gao, X.; Xu, B.; Weiss, P. S.; Zhao, Y. Chemistry and physics of a single atomic layer: strategies and challenges for functionalization of graphene and graphene-based materials. *Chem. Soc. Rev.* **2012**, *41*, 97–114.
- (8) Galashev, A. E.; Rakhmanova, O. R. Mechanical and thermal stability of graphene and graphene-based materials. *Physics-Uspokhi* **2014**, *57*, 970–989.
- (9) Lee, H.; Paeng, K.; Kim, I. S. A review of doping modulation in graphene. *Synthetic Metals* **2018**, *244*, 36–47.

- (10) Lee, R.; Jawad, Z.; Ahmad, A.; Chua, H. Incorporation of functionalized multi-walled carbon nanotubes (MWCNTs) into cellulose acetate butyrate (CAB) polymeric matrix to improve the CO₂/N₂ separation. *Process Safety and Environmental Protection* **2018**, *117*, 159–167.
- (11) Koenig, S.; Wang, L.; Pellegrino, J. Selective molecular sieving through porous graphene. *Nature Nanotech* **2012**, *7*, 728–732.
- (12) Wang, Y.; Yang, Q.; Li, J.; Yang, J.; Zhong, C. Exploration of nanoporous graphene membranes for the separation of N₂ from CO₂: a multi-scale computational study. *Phys. Chem. Chem. Phys* **2016**, *18*, 8352–8358.
- (13) Wang, S.; Dai, S.; en Jiang, D. Continuously Tunable Pore Size for Gas Separation via A Bilayer Nanoporous Graphene Membrane. *ACS Appl. Nano Mater* **2019**, *2*, 379–384.
- (14) Liu, H.; Daiab, S.; en Jiang, D. Insights into CO₂/N₂ separation through nanoporous graphene from molecular dynamics. *Science* **2013**, *5*, 9984–9987.
- (15) Cezar, H. M.; Lanna, T. D.; Damasceno, D. A.; Kirch, A.; Miranda, C. R. Revisiting greenhouse gases adsorption in carbon nanostructures: advances through a combined first-principles and molecular simulation approach. **Under Preparation**,
- (16) DELHOMMELLE, J.; MILLIÉ, P. Inadequacy of the Lorentz-Berthelot combining rules for accurate predictions of equilibrium properties by molecular simulation. *Molecular Physics* **2001**, *99*, 619–625.
- (17) Vekeman, J.; Faginas-Lago, N.; Cuesta, I. G.; Sánchez-Marín, J.; Merás, A. S. D. Nitrogen Gas on Graphene: Pairwise Interaction Potentials. *Computational Science and Its Applications – ICCSA 2018. ICCSA 2018* **2018**, 10964.
- (18) Yeamin, M. B.; Faginas-Lago, N.; Albertí, M.; Cuesta, I. G.; Sánchez-Marína, J.;

- de Merás, A. M. J. S. Multi-scale theoretical investigation of molecular hydrogen adsorption over graphene: coronene as a case study. *RSC advances* **2014**, *4*, 54447–54453.
- (19) Klimeš, J.; Bowler, D. R.; Michaelides, A. Chemical accuracy for the van der Waals density functional. *Journal of Physics: Condensed Matter* **2009**, *22*, 022201.
- (20) Cooper, V. R. Van der Waals density functional: An appropriate exchange functional. *Phys. Rev. B* **2010**, *81*, 161104.
- (21) Takeuchi, K.; Yamamoto, S.; Hamamoto, Y.; Shiozawa, Y.; Tashima, K.; Fukidome, H.; Koitaya, T.; Mukai, K.; Yoshimoto, S.; Suemitsu, M.; Morikawa, Y.; Yoshinobu, J.; Matsuda, I. Adsorption of CO₂ on Graphene: A Combined TPD, XPS, and vdW-DF Study. *Journal of Physical Chemistry C* **2017**, *121*, 2807–2814.
- (22) Shojaie, F.

N₂

- adsorption on the inside and outside the single-walled carbon nanotubes by density functional theory study. *Pramana - J Phys* **2018**, *90*, 54447–54453.
- (23) Humphrey, W.; Dalke, A.; Schulten, K. VMD – Visual Molecular Dynamics. *Journal of Molecular Graphics* **1996**, *14*, 33–38.
- (24) Kohlmeyer, A.; Vermaas, J.; Braun, E. akohlmey/topotools: Release 1.8. 2020; <https://zenodo.org/record/598373>.
- (25) Stukowski, A. Visualization and analysis of atomistic simulation data with OVITO—the Open Visualization Tool. *MODELLING AND SIMULATION IN MATERIALS SCIENCE AND ENGINEERING* **2010**, *18*.
- (26) Brenner, D. W.; Shenderova, O. A.; Harrison, J. A.; Stuart, S. J.; Ni, B.; Sinnott, S. B. A second-generation reactive empirical bond order (REBO) potential energy expression for hydrocarbons. *Journal of Physics: Condensed Matter* **2002**, *14*, 783–802.

- (27) Cornell, W. D.; Cieplak, P.; Bayly, C. I.; Gould, I. R.; Merz, K. M.; Ferguson, D. M.; Spellmeyer, D. C.; Fox, T.; Caldwell, J. W.; Kollman, P. A. A Second Generation Force Field for the Simulation of Proteins, Nucleic Acids, and Organic Molecules. *Journal of the American Chemical Society* **1995**, *117*, 5179–5197.
- (28) Mao, Z.; Garg, A.; Sinnott, S. B. Molecular dynamics simulations of the filling and decorating of carbon nanotubes. *Nanotechnology* **1999**, *10*, 273–277.
- (29) Huang, L.; Zhang, L.; Shao, Q.; Lu, L.; Lu, X.; Jiang, S.; Shen, W. Simulations of Binary Mixture Adsorption of Carbon Dioxide and Methane in Carbon Nanotubes: Temperature, Pressure, and Pore Size Effects. *The Journal of Physical Chemistry C* **2007**, *111*, 11912–11920.
- (30) Steele, W. A. The interaction of rare gas atoms with graphitized carbon black. *The Journal of Physical Chemistry* **1978**, *82*, 817–821.
- (31) Walther, J. H.; Jaffe, R.; Halicioglu, T.; Koumoutsakos, P. Carbon Nanotubes in Water: Structural Characteristics and Energetics. *The Journal of Physical Chemistry B* **2001**, *105*, 9980–9987.
- (32) Potoff, J. J.; Siepmann, J. I. Vapor–liquid equilibria of mixtures containing alkanes, carbon dioxide, and nitrogen. *AIChE Journal* **2001**, *47*, 1676–1682.
- (33) García-Pérez, E.; Parra, J.; Ania, C.; García-Sánchez, A.; van Baten, J.; Krishna, R.; Dubbeldam, D.; Calero, S. A computational study of CO₂, N₂, and CH₄ adsorption in zeolites. *Adsorption* **2007**, *13*, 469–476.
- (34) Vujić, B.; Lyubartsev, A. P. Transferable force-field for modelling of CO₂, N₂, O₂ and Ar in all silica and Na⁺ exchanged zeolites. *Modelling Simul. Mater.* **2016**, *24*, 1–26.
- (35) Murthy, C.; Singer, K.; Klein, M.; McDonald, I. Pairwise additive effective potentials for nitrogen. *Molecular Physics* **1980**, *41*, 1387–1399.

- (36) Hensley, A. J. R.; Kushal Ghale, C. R.; Dang, T.; Anderst, E. S.; Studt, F.; Campbell, C. T.; McEwen, J.-S.; Xu, Y. A DFT-Based Method for More Accurate Adsorption Energies: An Adaptive Sum of Energies from RPBE and vdW Density Functionals. *The Journal of Physical Chemistry C* **2017**, *121*, 4937–4945.
- (37) Berland, K.; Hyldgaard, P. Exchange functional that tests the robustness of the plasmon description of the van der Waals density functional. *Phys. Rev. B* **2014**, *89*, 035412.
- (38) Perdew, J. P.; Wang, Y. Accurate and simple analytic representation of the electron-gas correlation energy. *Phys. Rev. B* **1992**, *45*, 13244–13249.
- (39) Perdew, J. P.; Ruzsinszky, A.; Csonka, G. I.; Vydrov, O. A.; Scuseria, G. E.; Constantin, L. A.; Zhou, X.; Burke, K. Restoring the Density-Gradient Expansion for Exchange in Solids and Surfaces. *Phys. Rev. Lett.* **2008**, *100*, 136406.
- (40) Thompson, A. P.; Aktulga, H. M.; Berger, R.; Bolintineanu, D. S.; Brown, W. M.; Crozier, P. S.; in 't Veld, P. J.; Kohlmeyer, A.; Moore, S. G.; Nguyen, T. D.; Shan, R.; Stevens, M. J.; Tranchida, J.; Trott, C.; Plimpton, S. J. LAMMPS - a flexible simulation tool for particle-based materials modeling at the atomic, meso, and continuum scales. *Comp. Phys. Comm.* **2022**, *271*, 108171.
- (41) Jewett AI, S. D.; J, L.; SM, S.; OM, R.; M, R.; L, A.; M, M.; SM, B.; T, K.; RT, D.; J-E, S.; GJ, J.; DS, G. Moltemplate: A Tool for Coarse-Grained Modeling of Complex Biological Matter and Soft Condensed Matter Physics. *J. Mol. Biol.* **2021**, *433*, 166841.
- (42) Shah, J. K.; Marin-Rimoldi, E.; Mullen, R. G.; Keene, B. P.; Khan, S.; Paluch, A. S.; Rai, N.; Romanielo, L. L.; Rosch, T. W.; Yoo, B.; Maginn, E. J. Cassandra: An open source Monte Carlo package for molecular simulation. *Journal of Computational Chemistry* **2017**, *38*, 1727–1739.
- (43) Widom, B. Some Topics in the Theory of Fluids. *J. Chem. Phys.* **1963**, *39*, 1727–1739.

- (44) Gale, J. D. GULP: A computer program for the symmetry-adapted simulation of solids. *J. Chem. Soc., Faraday Trans.* **1997**, *93*, 629–637.
- (45) Vekeman, J.; Sánchez-Marín, J.; de Merás, A. S.; Cuesta, I. G.; Faginas-Lago, N. Flexibility in the Graphene Sheet: The Influence on Gas Adsorption from Molecular Dynamics Studies. *J. Phys. Chem. C* **2019**, *123*, 28035–28047.
- (46) Gordeev, E. G.; Polynskia, M. V.; Ananikov, V. P. Fast and accurate computational modeling of adsorption on graphene: a dispersion interaction challenge. *Physical Chemistry Chemical Physics* **2013**, *22*, 0.
- (47) Klimeš, J.; Michaelides, A. Perspective: Advances and challenges in treating van der Waals dispersion forces in density functional theory. *The Journal of Chemical Physics* **2012**, *120901*, 1–12.
- (48) Vidali, G.; Ihm, G.; Kim; Young, H.; W., C. M. Potentials of physical adsorption. *Surface Science Reports* **1991**, *12*, 135–181.
- (49) Artacho, E.; Anglada, E.; Diéguez, O.; Gale, J. D.; García, A.; Junquera, J.; Martin, R. M.; Ordejón, P.; Pruneda, J. M.; Sánchez-Portal, D.; Soler, J. M. The SIESTA method: developments and applicability. *Journal of Physics: Condensed Matter* **2008**, *20*, 064208.
- (50) Kumar, K. V.; Gadipelli, S.; Wood, B.; Ramisetty, K. A.; Stewart, A. A.; Howard, C. A.; Brett, D. J. L.; Rodriguez-Reinoso, F. Characterization of the adsorption site energies and heterogeneous surfaces of porous materials. *J. Mater. Chem. A* **2019**, *7*, 10104–10137.
- (51) Khalili, S.; Ghoreyshi, A. A.; Jahanshahi, M.; Davoodi, M. Experimental Evaluation of CO₂/N₂ Mixture Separation by Multi-multi-walled Carbon Nanotube. *Acta Physica Polonica A* **2013**, *123*, 230–232.

- (52) Rahimi, M.; Singh, J. K.; Babu, D. J.; Schneider, J. J.; Müller-Plathe, F. Understanding Carbon Dioxide Adsorption in Carbon Nanotube Arrays: Molecular Simulation and Adsorption Measurements. *The Journal of Physical Chemistry C* **2013**, *117*, 13492–13501.
- (53) Erdogan, F. O. Freundlich, Langmuir, Temkin and Harkins-Jura isotherms studies of H₂ adsorption on porous adsorbents. *Chemistry* **2019**, *13*, 129–135.